Investigation of the fracture characteristics of the interfacial bond between bone and cement: experimental and finite element approaches[†]

Fu-Tsai Chiang[1] and Jui-Pin Hung[2,*]

[1]*Department of Orthopedic, Taichung Armed Forces General Hospital, Taiwan, R.O.C.*
[2]*Department of Mechanical Engineering, National Chin-Yi University of Technology, Taiwan, R.O.C.*

.

Abstract

This study integrated the finite element method, fracture mechanics, and three-point bending test to investigate the fracture characteristics of the interfacial bond between bone and cement. The fracture tests indicated that the interfacial fracture toughness of the bone/cement specimens was 0.34 MN/m$^{3/2}$, with a standard deviation of 0.11 MN/m$^{3/2}$, which was in good agreement with the experimental data available in the literature. A finite element model of the experimental testing specimen was used to predict the critical stress intensity factor (SIF) at the fracture load by the proposed fracture analysis method. The critical SIF of the opening mode of the interface crack was 0.392 MN/m$^{3/2}$, which was slightly higher than the fracture toughness obtained in the experiment. Additionally, considering the coupled effects of the crack opening mode and shearing mode, the critical effective SIF was 0.411 MN/m$^{3/2}$, with a phase angle of 17.2°. Comparisons of the results obtained from the bending test and numerical analysis made it obvious that the fracture characteristics of the bonded interface between the bone and cement could be accurately predicted by the proposed model. With this analysis model, a realistic investigation on the debonding behavior of cemented artificial prosthetic components is highly expected.

Keywords: Bone/cement interface; Fracture toughness; Stress intensity factor

---

1. Introduction

Recently, the use of artificial prosthetic replacements has become an important surgical procedure in the orthopedic treatment of human joint diseases. The success of an artificial prosthetic procedure greatly depends on the fixation of the artificial prosthetic component after being implanted in the thighbone. Orthopedic clinical observations have found that cemented artificial prostheses fail due to the loosening of the implanted component after long-term usage. Numerous studies have shown that the cause of the loosening of the artificial stem was very complicated and multifaceted. The biological interaction between polyethylene wear debris and human bone might initiate bone resorptions and the subsequent fixation failure of the implanted stem [1-3]. In addition, deterioration of the bonded interfaces between the metal stem and cement mantle and between the bone and the cement mantle was the most immediate cause for the loosening of artificial prostheses [4-7].

In cemented artificial joints, the cement layers serve as the media to transmit the joint force from the metal stem to the thighbone. Since the bone cement is a porous, brittle material, tiny cracks can be generated at pore sites or cavities by the repeated cyclic stress induced under gait loadings. This has been found to result in local fatigue failure and fractures in the cement layers surrounding the stem [7]. As was observed in Cullteon [8], the stripped cracks on the fractured surface of retrieved bone cement clearly showed evidence of fatigue failure and the growth of cracks within the cement mantle. By conducting fatigue tests on cemented stem constructions, Topoleski [9] found that the fractured surface topography was similar to that observed on the retrieved cement. This revealed that bone cement in the human body would fail from fatigue fractures. Previous researches [7, 9] have made it clear that the gradual deterioration of the cement's bonding ability would give rise to the mechanical separation of the bone and cement, with such interfacial debonding behavior being ascribed to the propagation of cracks from interfacial defects along the bonded surfaces between the cement and bone. This also implied that the prolonged endurance of artificial prosthetic components was greatly dependent on the integrity of the bonded interface, associated with its mechanical properties.

In characterizing the interfacial mechanical properties of a bone/cement interface, experimental approaches have been the most frequently used methods, including tensile tests [10, 11] or push-in tests for measuring the tensile or shear strength [12-

14]. Such experimental configurations were often applied to evaluate factors affecting the bonding strength and the extent of their influence. Apart from the static strengths, interfacial fracture toughness is another important property that provides a bonding interface with the ability to resist the deterioration or debonding of the interfaces. From the viewpoint of fracture mechanics, the stress fields around a crack site can be quantified by the stress intensity factors of the crack tip. For composite structures bonded from dissimilar materials, a crack growth or substantial fracture along the interface is assumed to occur when the stress intensity factors at the interface crack tip, under various loading conditions, reaches the material's fracture toughness. Consequently, as a measure of the resistance to crack propagation, the interfacial fracture toughness of the bone/cement interface, rather than the interfacial bonding tension or shear strength, is regarded as the prominent property affecting its fatigue fracture life. Further, the growth of an interface crack will dominate the subsequent fatigue behavior of a cemented hip prosthesis and can be predicted by the Paris law [15], in which the effective stress intensity factors, rather than the tensile stress at crack sites, prevail as the characteristics of crack propagation. Therefore, these fracture parameters are of importance in determining the fracture behavior of a cemented prosthetic structure with interface defects or cracks. The search for ways to improve the interfacial properties of cement bonds, giving them higher fracture toughness, has thus become an imperative task in orthopedic biomaterial development.

Concerning this issue, the application of fracture mechanics to the measurement of interface bonding strength has been recognized as the preferred methodology to characterize interface integrity in the development of various orthopedic or dental composite biomaterials [16-18]. For example, ASTM E399-83 [19] regulated experimental configurations, using single edge notched beam (SENB) specimens for three-point bending tests and rectangular compact tension (RCT) specimens for tensile tests, to evaluate the material's fracture toughness or critical stress intensity factor. In these testing arrangements, the fracture behavior was dominated by the tensile opening crack mode. However, for a bone/cement bonded composite, the interfacial bonding strength has been experimentally measured to vary with the external loading mode, which is different from the tests under a pure tension or pure shear mode [20]. With mixed-mode dependent interfacial properties, especially the interfacial fracture toughness [21], the bonded interface would fail in a mixed mode from the coupled effects of an opening fracture mode (mode I) and in-plane shear fracture mode (mode II). For a three-dimensional cracked composite structure, the fracture behavior will become more complicated due to the effects of the loading modes on the inherent characteristics. When attempting to analyze the fracture behavior of an interfacial crack subjected to mixed loadings, it is necessary to take the three different cracking modes (the opening, shearing, and tearing modes) into consideration for an evaluation of the stress intensity fac-

tor. This is difficult when compared with a conventional approach, such as the crack opening displacement method, to a two-dimensional plane problem.

Therefore, the aim of this research was to develop a fracture analysis model for investigating the fracture characteristics of the bonded interface between bone cement and bovine cortical bone. To this purpose, we first conducted a series of three-point bending tests to measure the interfacial fracture properties of the bone/cement bonded specimens. Additionally, this study proposed a fracture analysis model to estimate the stress intensity factor of the interfacial crack by implementing the virtual crack closure technique into the three-dimensional finite element model. This numerical analysis mainly focused on the stress intensity factor variation at the crack tip with increasing loads. The results of the finite element predictions were compared with the experimental measurements to validate the proposed methodology for fracture analysis, which is expected to further an understanding of the interfacial debonding behavior of cemented artificial hip prostheses for future study.

2. Experimental work

2.1 Bone/cement specimen preparation

Fig. 1 shows the geometry of a rectangular bone/cement specimen based on ASTM E399-83 configuration. This bimaterial specimen has a total length of 60 mm, height of 10 mm, and thickness of 5 mm. The initial length of the interfacial crack is 3 mm. The cements used in this experiment were commercial acrylic cements with the following ingredients: (1) a liquid monomer that included Methyl Methacrylate, N-dimethyl pare-toluidine, and Hydroquinone, and (2) a powder containing Methyl Methacrylate-styrene copolymer, Polymethyl methacrylate, and Barium Sulphate. The preparation procedure for the bone/cement specimen can be briefly described as follows:

First, a piece of long bone was extracted from the mid-diaphysis region of a bovine tibia with a blade saw, the marrow contents were eliminated, and it was sliced into several segments with a cross sectional thickness of 4-8 mm. Each bone segment was then machined under a water spray to produce a rectangular sample. The surface to be bonded with cement was subjected to further wet grinding with sandpaper (＃800C) and the samples were stored in a freezer at -20°C for later use. To ensure that the bone/cement specimens were made under consistent conditions, all of the specimens were formed with a steel mold in a batch operation, 15 specimens at a time. The bone cement was prepared by mixing the powdered PMMA polymer with the liquid monomer in a container at room temperature following the manufacturer's guidelines. Then, after each bone sample was placed into a mold cavity, the bone cement was poured into the other side of the cavity and pressure was applied by hand to keep it well bonded with the bone. In addition, to form a pre-crack at the bonding inter-
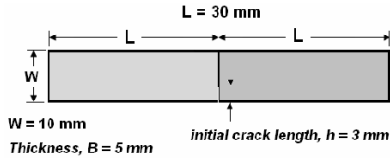
Fig. 1. Configuration of bone/cement bonded specimen for three-point bending test, h (=3mm) represents the initial length of interface crack.

face during specimen preparation, a thin piece of plastic tape with the proper dimensions was applied at the crack area to prevent the bone from bonding with the cement. After the bone cement polymerized, the specimens were carefully removed from the mold cavities and stored in a freezer at -20°C for testing.

2.2 Fracture toughness test

An Instron testing machine (model 4464) was used in the three-point bending test, as shown in Fig. 2. During testing, the upper crosshead imposed a compressive force on the specimen at a rate of 1.0 mm/min until the interfacial crack propagated to final fracture. From the load-displacement diagram recorded by the computerized data acquisition system, we can get the critical load F_{cr} at the onset of fracture. The interfacial fracture toughness K_{ic} can then be calculated according to Eq. (1),

$$K_{ic} = \frac{F_{cr} S \sqrt{W}}{BW^2} Y(\xi), \qquad \xi = h/W \tag{1}$$

where F_{cr} is the fracture load of the specimen, S is the span between the specimen's supports, h is the pre-crack length, and B and W are the thickness and height of the specimen, respectively. $Y(\xi)$ is the geometry function of the specimen [19], given by:

$$Y(\xi) = \frac{3\sqrt{\xi}(1.99 - \xi(1-\xi)(2.15 - 3.93\xi + 2.7\xi^2))}{2(1+2\xi)(1-\xi)^{3/2}} \tag{2}$$

3. Fracture modeling

3.1 Calculation of stress intensity factor

In this study, three-dimensional fracture mechanics was used to estimate the interfacial fracture toughness of bone/cement composite specimens. For a cracked material, the stress intensity factor at the crack tip will reach the propagation threshold when the bearing load increases to a certain critical value, at which time the internal crack will begin to grow. The fracture begins to occur when the crack tip stress intensity factor is equal to the fracture toughness of the material, i.e., $K_I = K_{IC}$. According to linear elastic fracture theory, the stress intensity factors (K_I, K_{II}, K_{III}) corresponding to three cracking modes (the opening mode, shearing mode, and twisting mode) can be related to the strain energy release rates
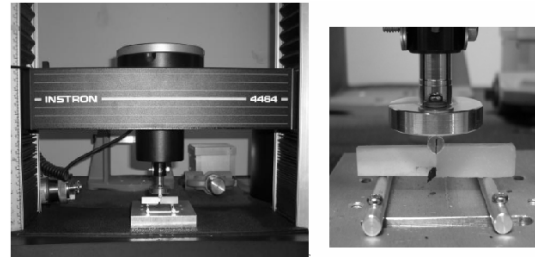

Fig. 2. Three-point bending test performed on Instron testing machine (Model 4464).

G_I, G_{II}, G_{III} at crack propagation by the following equations [22].

$$\begin{Bmatrix} G_I \\ G_{II} \\ G_{III} \end{Bmatrix} = \frac{1}{E_{eff}} \begin{Bmatrix} K_I^2 \\ K_{II}^2 \\ \frac{1}{2\mu} K_{III}^2 \end{Bmatrix} \tag{3}$$

In the above formulae, E_{eff} is the effective modulus and can be given as Eq. (4) for a three-dimensional problem according to Nikishkov and Atluri [23],

$$E_{eff} = E^* [\frac{1}{1-\mu^{*2}} + (\frac{\mu^*}{1+\mu^*})\frac{\varepsilon_{zz}}{\varepsilon_{xx} + \varepsilon_{yy}}] \tag{4}$$

$$\frac{1}{E^*} = \frac{(1-\mu_1^2)}{E_1} + \frac{(1-\mu_2^2)}{E_2} \quad , \quad \frac{1}{\mu^*} = \frac{1}{\mu_1} + \frac{1}{\mu_2} \tag{5}$$

where E^* and μ^* are the equivalent elastic modulus and Poisson's ratio of the bimaterial's structure, E_1, μ_1 and E_2, μ_2 are elastic modulus and Poisson's ratio of material 1 and material 2, respectively, and $\varepsilon_{xx}, \varepsilon_{yy}, \varepsilon_{zz}$ are the principal strains at the crack tip. Therefore, once the strain energy release rates for the crack tip are obtained, the stress intensity factors can be calculated from Eq. (3). In general, the strain energy release rates can be obtained by following the virtual crack closure technique (VCCT), which was modified and extended to a three dimensional structure by Shivakumar et al. [24], based on the crack closure integral proposed by Irwin [25] in 1957.

When the crack tip propagates by a tiny length Δa, the released strain energy can be estimated from the stress and displacement fields around the crack according to the integration,

$$G_i = \lim_{\Delta \to 0} \frac{1}{2t\Delta a} \int_0^t \int_0^{\Delta a} \sigma(r,s) \cdot w(\Delta a - r, s) dr ds , \tag{6}$$

where w is the crack opening displacement at the position (r,y) behind the crack front, t is the thickness of the crack surface, Δa is the crack length increment, and σ is the stress field of the crack's front surface. The strain energy released during the crack extension is equal to the energy required to close the crack to the state it was in before the extension. In the finite element model, the strain energy release rate can be calculated from the product of the nodal opening displacement and the
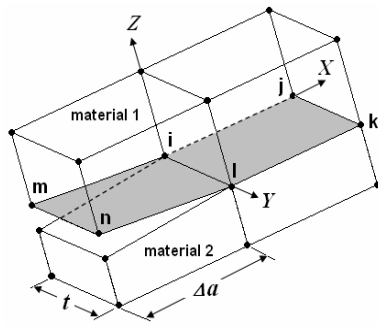
Fig. 3. Schematic of a cracked structure meshed with non-singular eight-node hexahedral elements, in which line *i-l* is the crack tip, surface *i-m-n-l* is the crack opening surface, *X*, *Y* is the tangent direction and *Z* is the normal direction of the opening surface, *t* is the thickness of crack, *Δa* is the crack extension.

nodal force of the elements around the crack front. According to Roeck [26], the strain energy release rate for a cracked structure meshed with non-singular eight node hexahedral elements (Fig. 3) can be expressed as,

$$G_I = \frac{1}{2t\Delta a}(F_{zi}w_m + F_{zl}w_n) , \qquad (7)$$

where G_I is the strain energy release rate, w_m and w_n are the relative opening displacements of nodes *m* and *n* at the crack opening surfaces along the Z axis, respectively, and F_{zi} and F_{zl} are the forces of nodes *I* and *l* at the crack front along the Z axis, respectively. Similar expressions for crack modes Ⅱ and Ⅲ can be expressed as follows:

$$G_{\mathrm{II}} = \frac{1}{2t\Delta a}(F_{xi}u_m + F_{xl}u_n) \qquad (8)$$

$$G_{\mathrm{III}} = \frac{1}{2t\Delta a}(F_{yi}v_m + F_{yl}v_n) \qquad (9)$$

For a bone/cement bonded composite with an interface crack, each of the nodal forces and nodal displacements in Eqs. (7) - (9) should take into account the difference in the nodal forces due to the difference in the stiffness of the materials on the upper and lower faces of the interface. Therefore, Eq. (7) has to be modified to:

$$G_I = \frac{1}{2t\Delta a}[(F_{zi}^1 w_m^1 + F_{zi}^1 w_n^1) + (F_{zi}^2 w_m^2 + F_{zi}^2 w_n^2)] , \qquad (10)$$

where w_m^1 and w_m^2 are the relative displacements for node *m* in material 1 and material 2, with respect to node *i*, respectively, and F_{zi}^1 and F_{zi}^2 are the nodal forces at node *i* calculated from the elements of material 1 and material 2, respectively. This is also valid for the calculation of the strain energy release rates of other cracking modes.

A cemented composite structure may experience complex loadings under normal working conditions or during other activities, enabling interfacial cracks to develop within the
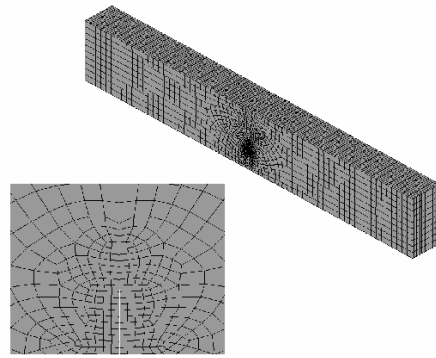

Fig. 4. Finite element model of bon/cement specimen, showing refined meshes around the crack tip.

cement bonded interfaces in a mixed fracturing mode, rather than in a single mode. It is therefore necessary to take the stress intensity factor of the different cracking modes into account when dealing with the crack propagation problem. The effective stress intensity factor K_{eff} for the cracking mode coupled with mode-I, mode-II, and mode-III can be expressed as [25]

$$K_{eff} = \sqrt{(K_I^2 + K_{II}^2) + (1+\nu)K_{III}^2} . \qquad (11)$$

In combination with mode-I and mode-II only, the effective stress intensity factor K_{eff} with the phase angle φ is of the form

$$K_{eff} = \sqrt{(K_I^2 + K_{II}^2)} \text{ and } \varphi = tan^{-1}\left(\frac{K_{II}}{K_I}\right) . \qquad (12)$$

3.2 Finite element crack modeling

Fig. 4 shows the finite element model of a bone-cement SENB specimen. The left side is cortical bone and the right side is acrylic bone cement. The interdigitation at the interface between the bone and cement was assumed to represent perfect bonding and a 3mm pre-crack was introduced at the edge of this interface. The FEM model was meshed with eight-node brick elements and consisted of a total of 19,860 elements and 22,784 nodes. Due to the presence of the interface crack, there was a square-root stress singularity at the crack front. Usually, a quarter-point singular element is used to model such a singular behavior in the stress fields. However, in the calculation of the stress intensity factor, it was demonstrated that the regular element yielded similar results to those of a model meshed with a singular element near the crack site [26]. The regular hexahedron brick elements were therefore adopted to refine the meshes around the crack site for further calculation of the stress intensity factors.

In addition, the bovine cortical bone and acrylic bone cement were modeled with a linear isotropic material model with elastic modules $E = 18.6$ GPa and 2.28 GPa, respectively, just as was used in [27]. Poisson's ratio for all of the materials was $\mu = 0.3$. To simulate the testing configuration, boundary
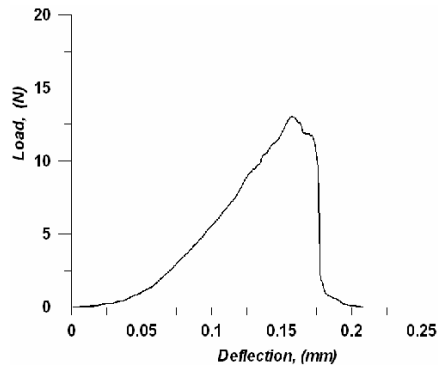
Fig. 5. The load-displacement diagram of the bone/cement specimen under three-point bending testing.

conditions were applied at the points where the specimen was supported and a compressive force was applied at the center point on the upper surface. Results of the FE static stress analysis were used to estimate the stress intensity factor variations with an applied load and then compared with experiment results.

4. Results

4.1 Fracture toughness of bone/cement interface

The bonding ability of bovine cortical bone and PMMA acrylic bone cement was characterized by the interfacial fracture toughness. For this, we conducted a series of three-point bending tests to evaluate the interfacial fracture toughness of the bimaterial composite specimens. Fig. 5 illustrates the relationship between the load and displacement of the bone/cement specimens under testing. It indicates that the bonded interface exhibited a nonlinear elastic behavior to some extent at the initial loading stage. After that, it showed a linear elastic behavior with an increase in the applied load. As the applied load was increased, the crack tip was driven to expand to final fracture. The average fracture load of the bone/cement specimens was approximately 12.3 N. The mean value of the interfacial fracture toughness K_{ic} was 0.34 MN/m$^{3/2}$, with a standard deviation of 0.11 MN/m$^{3/2}$. The fracture energy G_I corresponding to the mean fracture toughness was estimated as 50.68 J/m^2 according to the formula $G_I = K_{ic}^2 / E^*$, where E^* is the elastic modulus defined in Eq. (5). For comparison, the fracture properties of various bone/cement bonded specimens found in the literature are also summarized in Table 1.

4.2 Fracture analysis

This analysis was concerned with the variation in the stress intensity factor (SIF) at the interface crack tip with an increase in the loading, which was performed on specimen under loading conditions duplicated from the three-point bending test. Fig.6 shows the stress intensity factor at the interface crack tip as a function of the applied load, including opening fracture mode (crack mode I), shear fracture mode (crack mode II) and tearing fracture mode (crack mode III). As shown in Fig.6, the

Table 1. Comparisons of the fracture toughness and fractural energy for various bone/cement bonded interfaces.

Interface material compositions	Fracture toughness K_{ic}, (MN/m$^{3/2}$)	Fracture energy G_i, (J/m^2)
Bovine cortical bone + PMMA cement[a]	0.34±0.11	50.68±5.8 *
Bovine cortical bone + Fuji-II cement[b]	-	44.17±11.6
Bovine cortical bone + Fuji-IX cement[b]	-	52.98±8.5
Bovine cancellous bone + Fuji-I cement[c]	0.47±0.07	-
Bovine cancellous bone + Fuji-IX cement[c]	0.57±0.12	-
Bovine cancellous bone + PMMA cement[c]	0.62±0.16	-
Bovine femur bone + PMMA cement[d]	0.45~0.53	-

[a] Results obtained from current experiments.
* The fracture energy was estimated from fracture toughness according to the formula $G_I = K_{ic}^2 / E^*$.
[b] Results available in reference [28].
[c] Results available in reference [29].
[d] Results available in reference [30].

stress intensity factors increased with the load and the crack of mode I showed a higher SIF than the other two modes. As was found in the bending test, a critical fracture load of 12.3 N was measured for a bone/cement specimen. When the applied load reached this critical value, the mode-I SIF at the interface crack was estimated to be 0.392 MN/m$^{3/2}$, while the mode-II SIF and mode-III SIF were 0.123 and 0.04 MN/m$^{3/2}$, respectively. It was found that the mode-I SIF was slightly higher than the interfacial fracture toughness of the opening crack mode (0.34MN/m$^{3/2}$) measured in the three-point bending test. Under such a load, a rapid extension of the interface crack along the bonding surface of the bone/cement composite specimen could be anticipated, which might cause the whole bonded interface to separate in a brittle fracture manner. This result clearly indicated that the fracture analysis predicted a result consistent with that obtained in the three-point bending test.

Fig. 7 depicts the stress distribution around the crack site for a bone/cement specimen under an experimentally measured fracturing load of 12.3N. This also shows the shear distortion at the front surface of the interface crack because of the difference in the stiffness of the materials across the bonded interface. As implied in Fig. 7, the fracture phenomena that occurred in the bone/cement specimen under the loading mode of the three-point bending configuration were initiated primarily by the propagation of the interface crack in the opening mode, while the in-plane shear and out-of-plane tearing fracture modes were less significant. This may suggest that the effects of the shearing and tearing crack modes will become more apparent when the bonded specimen is subjected to a mixed loading. At this point, an equivalent stress intensity factor prescribing the coupled fracturing modes would be meaningful for realizing the initiation of the interfacial
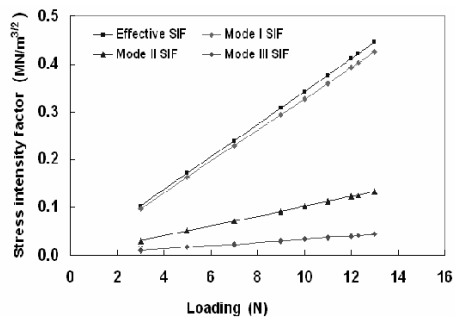
Fig. 6. Variation of stress intensity factors at interface crack tip with the increase of the applied load.
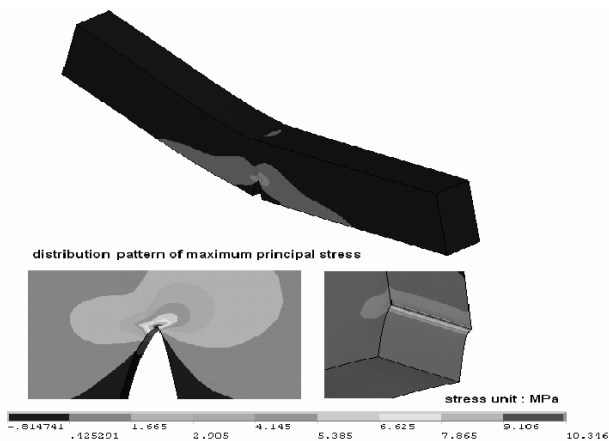

Fig. 7. Stress distribution of a deformed bone/cement specimen under experimental measured fracture load of 12.3N, showing a shear distortion at the interface crack, magnified by 200.

debonding failure. The mixed mode dependence of the interfacial mechanical properties was demonstrated in previous studies [20, 30]. As demonstrated in Wang and Agawal [30], the interfacial fracture toughness of bone/cement bonded structures measured using compact sandwich specimens (BCS) were scattered from 0.43 to 0.52 MN/m$^{3/2}$, while the associated mode mixity was characterized by a phase angle falling in the range of 11-17°. In the current study, the SENB testing arrangement was used to assess the interfacial fracture toughness of the bone/cement specimens. Generally, the interfacial fracture toughness measurements were quantified under the opening crack mode, which could not reflect the mixed mode conditions at the crack site. However, with the proposed fracture analysis, the mixed mode fracture characteristics of the interface crack were considered in the evaluation of the fracture toughness. Herein, the critical stress intensity factor for the combination of the mode-I opening and mode-II in-plane shearing was calculated as 0.416 MN/m$^{3/2}$, with a mixed mode phase angle of 17.4°. The current results demonstrate good agreement with the results reported in [30]. This also verifies that the fracture analysis model proposed in this study can supplement the insufficiency of the SENB experiment in quantifying the fracture characteristics of the interface between bone and cement.

5. Discussions

This study attempted to develop an interfacial fracture analysis model for investigating the interfacial fracture behavior of a bone/cement composite structure. The first step is to assess the fracture parameters of the interface between bone and cement. As presented in Table 1, the interfacial fracture strengths were scattered over a wide range, depending on the testing configuration used for the specimen, the bone segment scission and orientation, and the composition of the cement. These factors may contribute to the differences between the values in the literature and the present results, but with good consistency.

In the study by Lucksanasombool et al. [28], the fracture strength of bimaterial specimens formed with bovine cortical bone and Fuji cement were measured in terms of the fracture energy as 44.17±11.6 J/m^2 for Fuji-II cement and 52.98±8.5 J/m^2 for Fuji-IX cement, respectively. These measurements accord with the values estimated from current study (Table 1). Another study by Lucksanasombool et al. [29] verified that the interfacial fracture toughness of the bone/cement composite of SENB type could vary with the cement constituents. The mean values were reported as 0.47, 0.57 and 0.62 MN/m$^{3/2}$ for Fuji-I, Fuji-IX, and PMMA cement, respectively. In an experiment conducted by Wang and his colleagues [30], the compact specimens made from PMMA cement and bovine cortical bone were employed in a tensile test. The interfacial fracture toughness was measured across a range of 0.45~0.53 MN/m$^{3/2}$, which are also comparable to the current experimental measurements.

In the above comparison, it should be noted that the bone samples used in preparing the specimens were taken from different bovine bone sites, which caused the interfacial properties to have different values. According to Graham et al. [31], bone porosity was shown to have a significant effect on the interfacial strength of a bone and cement composite. In their study, the measured interfacial fracture toughness values were 1.15 MN/m$^{3/2}$ for dense bone with a low porosity and 1.46 MN/m$^{3/2}$ for bone with a high porosity, respectively. In addition, the results of Mann et al. [32] also verified that the interfacial bonding strength between femur bone and cement can be positively quantified by the amount of bone interdigitated with the PMMA cement. A recent experimental study by Arola et al. [33] also showed that the cement penetration volume can be increased by roughening the cortical bone surface, which indeed helps strengthen the interfacial mechanical properties. Consequently, with its greater porosity, the cancellous bone of the proximal femur was believed to achieve better interdigitation with bone cement as compared to cortical bone. As a result of its better mechanical binding effects, a high fracture energy for cancellous bone and cement composites was thus obtained in [31], as shown in Table 1. Additionally, to enhance the bonding ability, some improvements in cement preparation, such as mixing techniques associated with the different filling methods [34, 35], have also been devel-
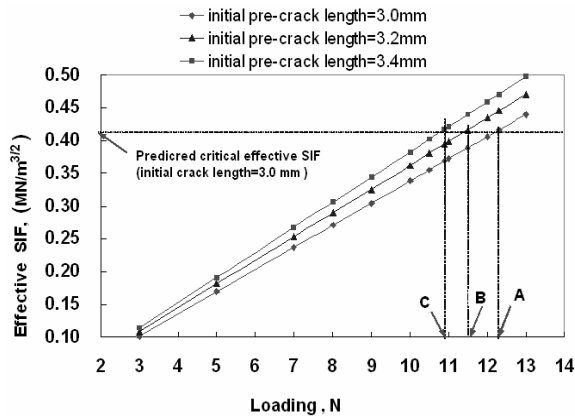
Fig. 8. Variation in the effective stress intensity factor of the interfacial crack with the applied load for three different bone/cement models with initial crack length of 3.0, 3.2 and 3.4 mm, respectively.

oped with the intention of increasing penetration of the cement into the bone [36, 37].

On the other hand, the marrow cavity of the femur bone is often shaped and brushed to different levels of surface roughness during the surgical procedure for prosthesis replacement [38]. This yields a wide variability in the integrity of the bone/cement interface [39], which is not only accompanied by differences in the localized bonding characteristics at this interface, but with strength differences in shearing and tension [39-41]. Such a regional variation in bonding properties might be why the clinical loosening failures of cemented prostheses behave in different manners. Meanwhile, this also highlights the influence of the variation in the bonding strength of the interface within the cemented component. In addition, previous studies have shown evidence of the presence of tiny voids or pores at the bone/cement interface within artificial joints [7-9]. These tiny defects could serve as initiation sites for interface cracks to propagate along the bonded surface of the cemented stem, thus causing extensive deterioration of the interface under follow-up gait loadings. As mentioned above, the crack parameters, such as the stress intensity factor at crack sites, rather than the interfacial tensile or shear stress, eventually govern the progression of these interfacial cracks.

The other objective of this study was to develop a fracture analysis model that could be applied to simulate the fracture behavior of a bone/cement interface within cemented prosthesis. As revealed in above-mentioned results, the fracture analysis model proposed in this study demonstrates good agreement with the results available in literatures.

With the proposed fracture analysis model, the effect of the initial crack size on the fracture resistance of the bonded interface was further realized by estimating the fracture load of bone/cement specimens with different interfacial crack lengths. In this analysis, in addition to the previous model with the 3.0 mm crack, two finite element models of bone/cement bonded specimens with initial cracks of 3.2 and 3.4 mm were created for the crack analysis. Fig. 8 shows the variation in the effective stress intensity factor of the interfacial crack with the ap-

plied load for the three different models. It can be seen that under the same load level a longer crack showed a higher stress intensity factor than a short one. Fig. 8 also shows the experimentally measured fracture load of 12.3 N for a bone/cement specimen with an interface pre-crack of 3.0 mm and the critical effective stress intensity factors associated with it, as indicated by the bold A and the horizontal dashed line. The critical effective stress intensity factor (0.416 MN/m$^{3/2}$) predicted in the above analysis was considered to be the fracture toughness of the interfacial crack with the mixed loading conditions that were induced under the bending test configuration. Therefore, the bone/cement finite element models with the 3.2 and 3.4 mm pre-cracks would be loaded to fracture when the effective stress intensity factors at the crack tip increased to the fracture toughness of the mixed mode. The critical fracture loads were estimated to be 11.5 and 10.8 N, herein indicated in the figure by the bold B and C, respectively. The mode–I fracture toughness values that corresponded to the fracture loads, as determined from the three-point bending experiment, were calculated to be 0.325 and 0.327 MN/m$^{3/2}$ for the initial crack lengths of 3.2 and 3.4 mm, respectively, according to Eq. (1)-(2). The estimated fracture load and mode-I fracture toughness values for the two cracks of different length were within the variance of these measured values. This seems to indicate that the initial crack size at the interface between the bone and cement has no direct influence on the interfacial fracture characteristic, but as revealed in results the fracture analysis results (Fig. 8), it does affect the load carrying capacity of the bonded specimen, and the subsequent crack development behavior.

In addition, for a bone/cement specimen under a fracturing load, the maximum tensile stress and shear stress generated within the bone material were 10.44 and 6.08MPa, respectively, and the maximum tensile stress and shear stress within the cement mantle were 10.7 and 3.29MPa, respectively. As to the whole specimen structure, the maximum stresses at the crack tip were 10.3MPa for tension and 4.5MPa for shear, respectively, and the maximum interfacial normal and shear stresses near the crack cite were 9.68MPa and 2.64MPa, respectively. A related study pointed out that the tensile strength of the interface between bovine cortical bone and PMMA cement was 1.13-5.75MPa and the shear strength was 2.36-6.5MPa [42]. Actually, the stress analysis showed that when the compressive load applied to the specimen model reached 7N, the interfacial normal stress at the bonded region near the crack site was 5.81Mpa, which is marginally above the interfacial tensile strength. Based on the static failure criteria, this may suggest that the bonded interface would probably begin to disintegrate from the initial crack by tensile stress, rather than shearing. The effective stress intensity factor at this loading instance was 0.24 MN/m$^{3/2}$. For a bonded specimen with an initial 3 mm long pre-crack, this effective SIF may be regarded as the threshold to initiate crack growth along the interface. After that, the subsequent development of interfacial fracture failure could be investigated from the extension of the

interfacial crack length associated with the crack tip stress intensity factor, which will increase with an increase in the applied load. But, this was not investigated in the current study.

In recent years, Verdonschot et al., [43], Colombi [44], Lennon et al., [45] and Perez et al. [46] have applied the finite element method to investigate fatigue failure in cemented hip prostheses. In their analysis models, continuum damage mechanics was used to quantify the cement failure behavior, while the interface failure was simulated based on static failure criteria [20]. In addition, the interfaces between the cement and bone or between the cement and stem were assumed to be in a completely bonded or completely debonded state during the entire simulation process. However, as revealed in the fatigue experiments conducted by McCormack [47], crack initiation and propagation within the cement mantle and the fatigue debonding of the interfaces actually dominated the failure of the cemented prosthetic component. The numerical study of Hung [48] also showed that fatigue damage to the cemented composite structures was first initiated at the proximal and distal regions, where a high tensile stress was generated, and then progressively propagated toward the remaining bonded regions under subsequent gait cycles. This fatigue failure rate was significantly affected by the localized debonding of the bone/cement interfaces [48]. The above studies obviously suggest that the interfacial debonding behavior is a long-term fatigue scenario contributed to by the propagation of interfacial cracks. Therefore, an analysis approach based on fracture mechanics would be more suitable for examining the interfacial failure process of the cemented prosthetic component, which was not considered in previous researches [43-46].

On the other hand, to simulate the interfacial fracture behavior of cemented prosthetic structures in a realistic manner, the establishment of an interfacial fracture analysis model is a prerequisite. Therefore, our goal was to develop an interface fracture analysis model by integrating the virtual crack closure technique with a finite element analysis model, by which we could evaluate the fracture parameters at the interface crack in three-dimensional space, rather than by using the conventional two-dimensional plane model adopted in [21, 49]. In addition, the extent of interfacial bonding extent has been shown to greatly affect the cement stress and failure probability of cemented hip prostheses [46, 48], while the interfacial properties of the bonded regions are critically affected by the depth of cement penetration into the bone [32]. Therefore, the modeling of the interfacial bonded state should appropriately reflect the real situation generated in a cemented structure. However, apart from the interface pre-crack, in the current FE model, the remaining regions of the bonding interfaces were also assumed to be completely bonded, forming a rigid bond, rather than an elastic bond, as in the case of the test specimen. Such an assumption would cause the interfacial stiffness to be higher than that of a realistic cemented structure, and hence the stress intensity factor under the fracturing load would be overestimated, resulting in a higher SIF than the experimentally measured fracture toughness.

From the current computational results with experimental verification, this study has successfully proposed a first step in developing a fracture analysis model for investigating the interfacial fracture behavior of a bone/cement composite structure. Nevertheless, to be a realistic analysis model, the actual interfacial stiffness at different bonded areas of the bone/cement interface, as well as the cement/stem interface, should be introduced into the finite element analysis model through the use of interface elements [50] with the experimentally measured interfacial properties [20,41]. In addition, time-variant interfacial bonded regions with local bonding characteristics should be implemented in the computational algorithm for simulating the evolution of the interfacial debonding failure with the gait loadings. In our future work on this issue, an interfacial fracture analysis model will be developed based on these concepts, and the effect of the extent of interfacial debonding on the fracture behavior will be taken into account. The accurate modeling of the interfacial mechanical behavior of cemented prosthetic components under physiological loading conditions can then be anticipated.

6. Conclusions

This study attempted to develop an interfacial fracture analysis model for investigating the interfacial fracture behavior of a bone/cement composite structure. To be a successful model for clinical application, interfacial properties that may vary with the bonding conditions, such as strength, stiffness, and fracture toughness, should be acquired from experiments with different testing configurations prior to the computational simulation. In this study, fracture experiments using a three-point bending test configuration were conducted to measure the fracture toughness of the bonded interface of PMMA cement and bovine cortical bone. A finite element fracture analysis model was also established based on linear elastic fracture mechanics and a virtual crack closure technique, with the purpose of estimating the fracture parameters of an interfacial crack. The proposed analysis model was verified to predict good results, comparable to the experimental measurements, achieving a first step in developing a fracture analysis model for the further study of cemented prostheses.

Nomenclature————————————

K_{ic}	:	Interfacial fracture toughness
F_{cr}	:	Fracture load of the specimen
S	:	Span between the specimen's supports
h	:	Length of pre-crack

|		
B, W	:	Thickness and height of the specimen
$Y(\xi)$	:	Geometry function of the specimen
G_I	:	Strain energy release rates for crack mode I
K_I	:	Stress intensity factor for crack mode I
E_i, μ_i	:	Elastic modulus and Poisson's ratio
w	:	Crack opening displacement
t	:	Thickness of the crack surface
Δa	:	Crack length increment
σ	:	Stress field of the crack's front surface
K_{eff}	:	Effective stress intensity factor
φ	:	Phase angle of crack

References

[1] W. H. Harris, The first 32 years of total hip arthroplasty: one surgeon's perspective. *Clinical Orthopaedics and Related Research*, 274 (1992) 6-11.

[2] C. G. Mohler, J. J. Callaghan, D. K. Collis and R. C. Johnston, Early loosening of the femoral component at the cement-prosthesis: interface after total hip replacement. *The Journal of Bone and Joint Surgery*, 77A (1995) 1315-1322.

[3] H. C. Amstutz and P. Campbell, Mechanism and clinical significance of wear debris-induced osteolysis. *Clinical Orthopaedics and Related Research*, 276 (1992) 7-18.

[4] M. Jasty, W. J. Maloney, C. R. Bradgon, T. Haire and W. H. Harris, Histomorphological studies of the long-term skeltal responses to well fixed cemented femoral components. *The Journal of Bone and Joint Surgery*, 72 (1990) 1220-1229.

[5] N. Verdonschot and R. Huiskes, Cement debonding process of total hip arthroplasty stems. *Clinical Orthopaedics and Related Research,* 336 (1997) 297-307.

[6] R. P. Robinson, T. P. Lovell, T. M. Green and G. A. Baliey, Early femoral component loosening in DF-80 total hip arthroplasty. *Journal of Arthroplasty*, 4 (1989) 55-64.

[7] M. Jasty, W. J. Maloney, C. R. Bradgon, D. O'Connor, T. Haire and W. H. Harris, The initiation of failure in cemented femoral components of hip arthoplasties. *The Journal of Bone and Joint Surgery*, 3B (1991) 551-558.

[8] T. P. Culleton, P. J. Prendergast and D. Taylor, Fatigue failure in the cement mantle of an artificial hip joint. *Clinical Material*, 12 (1993) 95-102.

[9] L. D. T. Topoleski, P. Ducheyne and J. M. Taylor, A fractographic analysis of in vivo polymethlmethacrylate bone cement failure mechanism. *Journal of Biomedical Materials Research*, 24 (1990) 145-154.

[10] K. A. Mann, D. C. Ayers, F. W. Werner, R. J. Nicoletta and M. D. Fortino, Tensile strength of the cement-bone interface depends on the amount of the bone interdigitation with PMMA cement. *Journal of Biomechanics*, 30 (4) (1997) 339-346.

[11] K. Masaki, T. Jiro, S. Shuichi, K. Keiichi, N. Masashi and K. Tadashi, Interfacial tensile strength between polymethylmethacrylate based bioactive bone cement and bone. *Journal of Biomedical Materials Research,* 63 (5) (2002) 564-571.

[12] M. Ogiso, M. Yamaura, P. T. Kuo, D. Borgese and T. Matsumoto, Comparative push out test of dense HA implant and HA coated implanted: findings in a canine study. *Journal of Biomedical Materials Research*, 39 (1998) 364-372.

[13] J. Li, H. Liao, B. Fartash, L. Hermansson and T. Johson, T. Surface dimpled commercially pure titanium implant and bone ingrowth. *Biomaterials*, 18 (1997) 691-696.

[14] S. Wang, W. R. Lacefield and J. E. Lemons, Interfacial shear strength and histology of plasma sprayed and sintered hydroxyapatite implants in vivo. *Biomaterials*, 17 (1996) 1945-1970.

[15] P. C. Paris and F. A. Erdogan, A critical analysis of crack propagation laws. *Trans ASME J Basic Engineering*, 58D (1963) 528-534.

[16] M. Zor, M. Kucuk and S. Aksoy, Residual stress effects on fracture energies of cement-bone and cement-implant interfaces. *Biomaterials*, 23 (7) (2002) 1595-1601.

[17] B. H. Miller, H. Nakajima, J. M. Powers and M. E. Nunn, Bond strength between cements and metals used for endodontic posts. *Dental Materials*, 14 (5) (1998) 312-320.

[18] D. H. Pashley, H. Sano and B. Ciucchi, Adhesion testing of dentin bonding agents: A review. *Dental Materials*, 11 (1998) 312-320.

[19] American Society for Testing and Materials (ASTM), Standard E399-83, Standard test methods for plane strain fracture toughness and strain energy released rate of plastic materials. *Annual Book of ASTM Standards*, 1987.

[20] K. A. Mann, R. Mocarski, L. A. Damron, M. J. Allen and D. C. Ayers, Mixed-mode failure response of the cement-bone interface. *Journal of Orthopedic Research*, 19 (6) (2001) 1153-1161.

[21] N. Choupani, Interfacial mixed-mode fracture characterization of adhesively bonded joints. *International Journal of Adhesion and Adhesives*, 28 (6) (2008) 267-282.

[22] S. Yang and F. G. Yuan, Determination and representation of the stress coefficient terms by path-independent integrals in anisotropic cracked solids. *International Journal of Fracture*, 101 (2000) 291-319.

[23] G. P. Nikishkow and S. N. Atluri, Calculation of fracture mechanics parameters for an arbitrary three-dimensional crack, by equivalent domain integral method. *International Journal for Numerical Methods in Engineering*, 24 (9) (1987)1801-1821.

[24] K. N. Shivakumar and J. C. Newman, ZIP3D – an elastic and elastic-plastic finite-element analysis program for cracked bodies. *Technical memorandum NASA-TP-102753*. June, 1990.

[25] G. R. Irwin, Analysis of stresses and strains near the end of a crack traversing a plate. *Journal of Apply Mechanics*, 24 (1957) 361-364.

[26] G. De Roeck and M. M. Abdel Wahab, Strain energy release rate formulae for 3D finite element. *Engineering Fracture Mechanics*, 50 (4) (1995) 569-580.

[27] K. A. Mann, D. L. Bartel, T. M. Wright and A. H. Burstein, Coulomb frictional interfaces in modeling cemented total hip replacements: a more realistic model. *Journal of Biomechanics*, 28 (9) (1995) 1067-1078.

[28] P. Lucksanasombool, W. A. J. Higgs, R. J. E. D. Higgs and M. V. Swain, Interfacial fracture toughness between bovine cortical bone and cements. *Biomaterials*, 24 (2003)1159-1166.

[29] P. Lucksanasombool, W. A. J. Higgs, M. Ignat, R. J. E. D. Higgs and M. V. Swain, Comparison of failure characteristics of a range of cancellous bone-bone cement composites. *Journal of Biomedical Materials Research*, 64 (1) (2003) 93-104.

[30] X. Wang and C. M. Agrawal, Interfacial fracture toughness of tissue-biomaterial systems. *Journal of Biomedical Materials Research*, 38 (11) (1997) 1-10.

[31] J. Graham, M. Ries and L. Pruitt, Effect of Bone Porosity on the Mechanical Integrity of the Bone-Cement Interface. *The Journal of Bone and Joint Surgery*, 85 (10) (2003) 1901-1909.

[32] K. A. Mann, D. C. Ayers, F. W. Werner, R. J. Nicoletta and M. D. Fortino, Tensile strength of the cement-bone interface depends on the amount of the bone interdigitation with PMMA cement. *Journal of Biomechanics*, 30 (4) (1997) 339-346.

[33] D. Arola, K.A. Stoffel and D. T. Yang, Fatigue of the cement/bone interface: the surface texture of bone and loosening. *Journal of Biomedical Materials Research*, 76 (2) (2006) 287-297.

[34] C. S. Oishi, R. H. Walker and C. W. Colwell, The femoral component in total hip arthroplasty. Six to eight-year follow-up of one hundred consecutive patients after use of a third-generation cementing technique**.** *The Journal of Bone and Joint Surgery*, 76 (8) (1994) 1130-1136.

[35] W. F. Mulroy, D. M. Estok and W. H. Harris, Total hip arthroplasty with use of so-called second-generation cementing techniques. A fifteen-year-average follow-up study. *The Journal of Bone and Joint Surgery*, 77 (12) (1995) 1845-1852.

[36] W. MacDonald, E. Swarts and R. Beaver, Penetration and shear strength of cement-bone interfaces in vivo. *Clinical Orthopaedics and Related Research*, 286 (1993) 283-288.

[37] M. M. Panjabi, V. K. Goel, H. Drinker, J. Wong, G. Kamire and S. D. Walter, S. D. Effect of pressurization on methylmethacrylate-bone interdigitation: an in vitro study of canine femora. *Journal of Biomechanics*, 16 (7) (1983) 473-480.

[38] R. S. Majkowski, A. W. Milles and G. C. Bannister, Bone surface preparation in cemented joint replacement. *The Journal of Bone and Joint Surgery*, 75 (B) (1993) 459-463

[39] K. M. Oates, D. L. Barrera, W. N. Tucker, C. C. Chau, W. D. Bugbee and F. R. Convery, In vivo effect of pressurization of polymethylmethacrylate bone-cement. Biomechanical and histological analysis. *Journal of Arthroplasty*, 10 (3) (1995) 373-381.

[40] D. J. Bean, F. R. Convery, S. L. Woo and R. L. Lieber, Regional variation in shear strength of the bone-polymethylmethacrylate interface. *Journal of Arthroplasty*, 2 (4) (1987) 293-298.

[41] K. A. Mann, F. W. Werner and D. C. Ayers, Mechanical strength of the cement-bone interface is greater in shear than in tension. *Journal of Biomechanics*, 32 (11) (1999) 1251-1254.

[42] X. Wang, A. Subramanian, R. Dhanda and M. Agrawal, Testing of bone-biomaterial interfacial bonding strength: a comparison of different techniques. *Journal of Biomedical Materials Research*, 33 (1996) 133–138.

[43] N. Verdonschot and R. Huiskes, The effect of cement-stem debonding in THA on the long-term failure probability of cement. *Journal of Biomechanics*, 30 (8) (1997) 795-802.

[44] P. Colombi, Fatigue analysis of cemented hip prosthesis: damage accumulation scenario and sensitivity analysis. *International Journal of Fatigue*, 24 (2002) 739-746.

[45] B. Lennon, B. A. O. McCormack and P. J. Prendergast, The relationship between fatigue and implant surface finish in proximal femoral prostheses. *Medical Engineering & Physics*, 25 (2003) 833-841.

[46] M. A. Perze, J. Grasa, J. M. Garica-Aznar, A. Beaj and M. Doblare, Probabilistic analysis of the influence of the bonding degree of the stem-cement interface in the performance of cemented hip prostheses. *Journal of Biomechanics*, 39 (2006) 1859-1872.

[47] B. A. O. McCormack, P. J. Prendergast and D. G. Gallagher, Experimental study of damage accumulation in cemented hip prostheses. *Clinical Biomechanics*, 11 (1996) 214-219.

[48] J. P. Hung, J. S. S.Wu and J. H. Chen, Effects of interfacial debonding on fatigue Damage of cemented hip prosthesis. *Journal of the Chinese Institute of Engineer,* 26 (4) (2003) 791-801.

[49] X. Wang and C. M. Agrawal, A mixed mode fracture toughness test of bone-biomaterial interfaces. *Journal of Biomedical Materials Research*, 53 (2003) 664-672.

[50] M. S. Alam and M. A. Wahab, Modeling the fatigue crack growth and propagation life of a joint of two elastic materials using interface elements. *International Journal of Pressure Vessels & Piping*, 82 (2005) 105-113.

Fu-Tsai Chiang received the M.D. degrees from National Defense Medical Center, Taipei, Taiwan in 1992, respectively, and his HAMD degree from ASIA University, Taiwan in 2008. Dr. Chiang is currently an Attending Physician at the Department of Orthopedic, Taichung Armed Force General Hospital, in Taiwan. His research interests are in the area of failure analysis of artificial prosthetic components and orthopedic biomechanics.
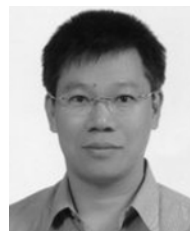
Jui-Pin Hung received the B.S. and M.S. degrees in Mechanical Engineering from National Chiao Tung University, Hsinchu, Taiwan in 1981 and 1983, respectively, and his Ph.D. degree from National Chung Hsing University in 2002. Dr. Hung is currently an associate professor at the Department of Mechanical Engineering at Chin Yi University of Technology in Taichung County, Taiwan. His research interests are in the area of machine tool design, failure analysis of mechanical components and orthopedic biomechanics.